Kilohertz alternating current neuromodulation of the pudendal nerves: effects on the anal canal and anal sphincter in rats

Coolen, R.L.; Emmer, K.M.; Spantidea, P.I.; Asselt, E. van; Scheepe, J.R.; Serdijn, W.A.; Blok, B.F.M.

DOI
10.32725/jab.2022.009

Publication date
2022

Document Version
Final published version

Published in
Journal of Applied Biomedicine

J Appl Biomed
DOI: 10.32725/jab.2022.009
journal homepage: http://jab.zsf.jcu.cz

Journal of Applied Biomedicine

Original research article

Kilohertz alternating current neuromodulation of the pudendal nerves: effects on the anal canal and anal sphincter in rats

Rosa L. Coolen [1] *, Koen M. Emmer [2], Panagiota I. Spantidea [1], Els van Asselt [1], Jeroen R. Scheepe [1], Wouter A. Serdijn [2], Bertil F. M. Blok [1]

[1] *Erasmus Medical Center, Department of Urology, Rotterdam, Zuid-Holland, Netherlands*
[2] *Delft University of Technology, Section Bioelectronics, Delft, Zuid-Holland, Netherlands*

Abstract
The first two objectives were to establish which stimulation parameters of kilohertz frequency alternating current (KHFAC) neuromodulation influence the effectiveness of pudendal nerve block and its safety. The third aim was to determine whether KHFAC neuromodulation of the pudendal nerve can relax the pelvic musculature, including the anal sphincter. Simulation experiments were conducted to establish which parameters can be adjusted to improve the effectiveness and safety of the nerve block. The outcome measures were block threshold (measure of effectiveness) and block threshold charge per phase (measure of safety). *In vivo*, the pudendal nerves in 11 male and 2 female anesthetized Sprague Dawley rats were stimulated in the range of 10 Hz to 40 kHz, and the effect on anal pressure was measured. The simulations showed that block threshold and block threshold charge per phase depend on waveform, interphase delay, electrode-to-axon distance, interpolar distance, and electrode array orientation. *In vivo*, the average anal pressure during unilateral KHFAC stimulation was significantly lower than the average peak anal pressure during low-frequency stimulation ($p < 0.001$). Stimulation with 20 kHz and 40 kHz (square wave, 10 V amplitude, 50% duty cycle, no interphase delay) induced the largest anal pressure decrease during both unilateral and bilateral stimulation. However, no statistically significant differences were detected between the different frequencies. This study showed that waveform, interphase delay and the alignment of the electrode along the nerve affect the effectiveness and safety of KHFAC stimulation. Additionally, we showed that KHFAC neuromodulation of the pudendal nerves with an electrode array effectively reduces anal pressure in rats.

Keywords: Anal sphincter; Electrical stimulation; High-frequency neuromodulation; Neurostimulation; Pelvic floor; Pudendal nerves

Highlights:
- KHFAC effectiveness depends on: waveform, interphase delay, electrode position.
- Block threshold charge per phase is an important outcome in KHFAC design.
- Pudendal KHFAC neuromodulation effectively decreases anal pressure in rats.
- Pudendal KHFAC can potentially treat dyssynergic defecation.

Introduction

The pelvic floor is a complex muscular apparatus that serves three important functions, namely, defecation, micturition, and sexual function (Rao and Patcharatrakul, 2016). The neural control of these three functions has common pathways. For example, the motor control is executed through nerve fibers in the pudendal nerve. Dysfunction can result in disorders such as urinary retention, dyssynergic defecation, and perineal and anal pain. Dyssynergic defecation is a common condition to which 25% of chronic constipation can be attributed (Nyam et al., 1997). Many alternative descriptions exist, such as anismus, obstructed defecation, and pelvic floor dyssynergia (Bharucha et al., 2006; Lembo and Camilleri, 2003). Most patients with dyssynergic defecation exhibit an inability to relax the external anal sphincter (EAS) during defecation. Usually, this problem consists either of an impaired rectal contraction, a paradoxical contraction of the anal muscles during defecation, including the EAS, or the anal muscles do not relax enough. About 61% of patients with dyssynergic defecation exhibit impaired rectal contraction during anorectal manometry (Rao et al., 1998). Paradoxical anal contraction was shown to be present in 78% of patients with dyssynergic defecation (Rao et al., 1998).

Dyssynergic defecation bears particular resemblance to non-obstructive urinary retention and detrusor sphincter

* **Corresponding author:** Rosa L. Coolen, Erasmus Medical Center, Department of Urology, Room Na-1524, Doctor Molewaterplein 40, 3015 GD Rotterdam, Netherlands; e-mail: r.coolen@erasmusmc.nl
http://doi.org/10.32725/jab.2022.009
Submitted: 2021-11-16 • Accepted: 2022-05-23 • Prepublished online: 2022-06-21
J Appl Biomed 20/2: 56–69 • EISSN 1214-0287 • ISSN 1214-021X

dyssynergia, a condition in which the coordination between the bladder and the external urethral sphincter (EUS) is lost. This results in an inability to void because the sphincter does not relax (enough) while the bladder is contracting. The most common first-line treatment of both dyssynergic defecation and non-obstructive urinary retention is pelvic floor physical therapy with biofeedback (Rao et al., 2016). However, this treatment is not effective in all patients and often significant impairment of health-related quality of life remains (Rao and Patcharatrakul, 2016). Furthermore, low-frequency electrical stimulation is widely used as a treatment option for non-obstructive urinary retention, but it has limited effectiveness (Coolen et al., 2020). Therefore, there is a need for other treatment options.

During micturition or defecation, the EUS or EAS must relax in order to empty the bladder or the rectum. Both sphincters are innervated by the pudendal nerve, therefore this nerve provides a target for electrical stimulation therapy in the treatment of functional bladder and bowel disorders. A specific type of electrical neuromodulation, kilohertz-frequency alternating-current (KHFAC) neuromodulation, is hypothesized to cause nerve conduction block in peripheral nerves and, therefore, relaxation of the target muscle. When applying this type of stimulation, an immediate onset response occurs. This onset response consists of repetitive nerve firing, and might induce a transient muscle twitch or pain (Miles et al., 2007). Thus far, few attempts have been made to apply KHFAC neuromodulation without an onset response. In one approach the amplitude was decreased below block threshold after nerve block was established to avoid a second onset response when increasing the amplitude to block threshold again to establish serial nerve blocks (Bhadra et al., 2009). Another approach is the design of waveforms that cause sodium channel inactivation without prior activation, and thus eliminating the onset response (Yi and Grill, 2020). High-frequency stimulation of the pudendal nerve to achieve nerve blockage and relaxation of the EUS has been studied previously in several animal models by using cuff electrodes. It has been shown to temporarily relax the EUS, enabling voiding (Bhadra et al., 2006; Cai et al., 2019; Tai et al., 2007). However, no evidence exists on the effects of high-frequency electrical nerve blockage with electrode arrays (leads) of the pudendal nerve on the anal sphincter. To design a successful KHFAC neuromodulation therapy for the pudendal nerve, it is necessary to understand what impact different stimulation parameters have on efficacy, safety and power efficiency. Therefore, we tested earlier researched KHFAC stimulation parameters against a new quality measure, studied the impact of new waveform alterations, and studied how bipolar electrode design can improve KHFAC therapy. Important outcomes are "block threshold" and the "block threshold charge per phase". The latter outcome measure reflects the charge that is injected into the tissue during stimulation, and thus indirectly reflects the safety of the stimulation.

The aim of this study was to determine which parameters of KHFAC neuromodulation influence the effectiveness and safety of the nerve block, and to determine whether KHFAC neuromodulation of the pudendal nerves with a commercially available electrode array can relax the pelvic musculature, including the anal sphincter in rats.

Materials and methods

This study consisted of two parts. The first part focused on *in silico* experiments in which the influence of multiple parameters on the block threshold and block threshold charge per phase of KHFAC neuromodulation were simulated. The second part consisted of animal experiments in which the effects of KHFAC neuromodulation of the pudendal nerve on anal pressure were evaluated in anesthetized rats.

Simulations

The McIntyre–Richardson–Grill (MRG) model provides an axon model of myelinated mammalian axons based on human data (McIntyre et al., 2002). We chose an axon diameter of 10 μm, based on an estimate of the diameter of the human pudendal nerve. This axon diameter resulted in the MRG model parameters shown in Suppl. A Table 1. The simulation environment Neuron was chosen (Hines and Carnevale, 1997). The simulations were performed in the simulation platform Brainframe (Smaragdos et al., 2017). The following parameters were studied: waveform, interphase delay, electrode-to-axon distance, electrode array (lead) orientation, and interpolar distance.

The performance of these parameters was compared by looking at two quality measures:

- Block threshold: this is the minimum current (or voltage) amplitude required to create a successful nerve block in the set of stimulating conditions.
- Block threshold charge per phase: this is the charge carried by a single anodic or cathodic pulse when the current amplitude is equal to the block threshold. This charge is dependent on the surface area under the anodic or cathodic (current or voltage) pulse. The charge per phase is an important parameter when evaluating safety, as building up too much charge at the electrode-tissue-interface can lead to irreversible reactions (Merrill et al., 2005). It also provides a more realistic view on what is physically happening than the amplitude itself, as the charge per phase is a measure of the maximum number of electrons that are actually injected into the tissue.

A monopolar simulation set-up was used for assessing the effect of waveform alterations and interphase delay on block threshold and block threshold charge per phase (Suppl. A Table 2). The following waveform alterations were assessed:

- A sine wave, square wave, and triangle wave current, for the frequency 3 kHz, and the frequencies from 4 kHz until 40 kHz with 2 kHz intervals (thus: 3 kHz, 4 kHz, 6 kHz, 8 kHz, ..., 38 kHz, 40 kHz).
- A square wave current with interphase-delays; the interphase delays are short periods of time between the positive and negative phase of the waveform, or vice-versa, during which the signal is constant at a value of $(I_{high}+I_{low})/2$, I_{high} being the maximum positive magnitude of the stimulation current and I_{low} being the minimum negative magnitude of the stimulation current, respectively. For the simulations, the interphase delays are introduced to a 10 kHz signal. The interphase delay following the anodal pulse (defined as the anodal interphase delay $T_{ipd,anodal}$), and the cathodal interphase delay (defined as the cathodal interphase delay $T_{ipd,cathodal}$) are both varied from 0% to 90% with steps of 5% (or 0.01 ms to 0.09 ms with steps of 0.005 ms), with $T_{ipd,anodal} + T_{ipd,cathodal} \leq 90\%$.

A bipolar simulation set-up was used to assess the effect on effectiveness of both the orientation of the electrode with regard to the axon and the distance between the two poles (interpolar distance) (Suppl. A Table 3). Additional information can be found in Suppl. B.

Experimental procedures

Guidelines of the local Animal Experiment Committee for animal experiments were followed. The animals were housed in a facility with a 12 h light/dark cycle and given free access to food and water. A total of 13 Sprague Dawley rats (11 male and 2 female) with a mean weight of 431 g ± 105 g (range: 313–616 g) and a mean age of 12 weeks ± 2 weeks (range: 9–18 weeks) were used. The animals were anesthetized with urethane (50% solution, 1.2–1.5 g/kg) of which two-thirds was injected i.p. and one-third s.c. (van Asselt et al., 2017). After induction of anesthesia, the rat was placed on a heated pad, in a prone position. A dorsal midline incision was made at the L6–S1 level, and the sciatic nerve was localized on both sides. The compound pudendal nerve was then dissected at the point where it enters the space between the sacrum and the hip bone. Two ring electrode arrays (quadripolar leads, Axonics, Irvine, CA, USA, Fig. 1b and Fig. 1c) were placed parallel along the left and right pudendal nerves. A proximal and a distal electrode array were placed alongside each pudendal nerve (Fig. 1c). The proximal electrode array was used for low frequency stimulation and the distal electrode array was used for KHFAC stimulation. Two of the four poles were connected to a stimulator device (custom made by the Section Bioelectronics of Delft University of Technology). This stimulator offers charge-balanced voltage stimulation and has two output channels that both can deliver low-frequency and high-frequency (in the kilohertz range) stimulation with programmable waveform, amplitude, pulse width/duty cycle, pulse repetition frequency, interpulse delay, and interphase delay (Fig. 1a, d, e). The output of the stimulator was verified with a Tektronix TDS2014C four-channel oscilloscope prior to conducting the *in vivo* experiments. In the case of the bilateral stimulations, two additional stimulators (Hameg HM 8130 and SI-Heidelberg) were used to deliver low-frequency stimulation on both sides.

A balloon catheter (6 Fr, Folysil, Coloplast) filled with 1 ml of water was inserted into the anal canal. The catheter was attached to a disposable pressure transducer. The anal pressure was measured using a Statham SP1400 blood pressure monitor (Gould Inc., Oxnard, CA, USA). At the end of the experiment, the rat was euthanized with an overdose of KCl, injected into the heart.

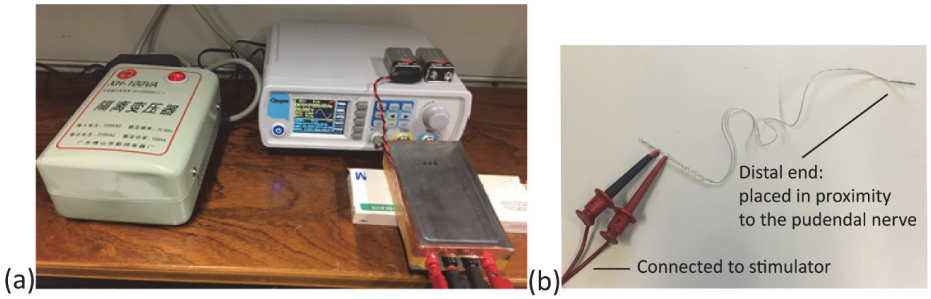

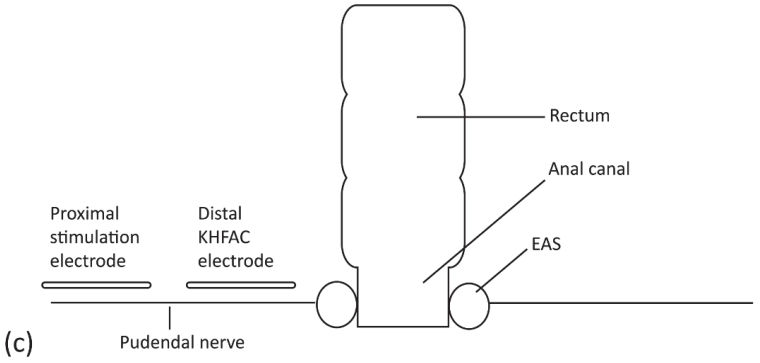

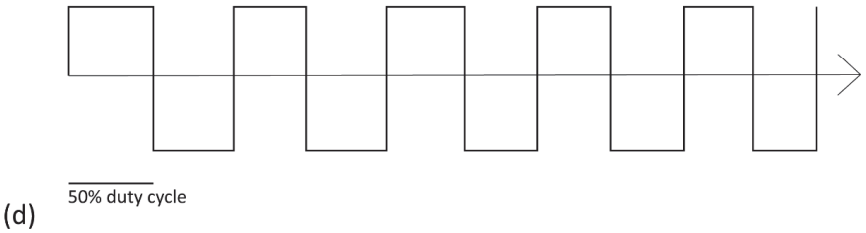

(e)

Frequency	0 - 800 kHz
Amplitude	1 mV - 10 V
Duty cycle	0.1 - 99.9 %
Waveform	sine, square, pulse, triangle

Fig. 1. (**a**) The external stimulator. (**b**) Electrode array. (**c**) Schematic representation of electrode placement. (**d**) Square waveform with a 50% duty cycle, thus the cathodic and anodic phases are of the same duration. (**e**) Stimulation characteristics of the external stimulator. EAS = external anal sphincter; KHFAC = kilohertz frequency alternating current.

Electrical stimulation

Low-frequency voltage stimulation was carried out at frequencies of 10, 20 and 30 Hz. Different amplitudes were used: 1, 2, 3, 4, and 5 volt (V). A square waveform with a duty cycle of 20% with no interphase delay was used. These low-frequency stimulation experiments were performed to establish which frequency should be used for activation of the pudendal nerve. Additionally, several durations of low-frequency stimulation were applied to determine after which duration the anal sphincter muscles fatigue. High-frequency stimulation was carried out at frequencies of 3, 5, 10, 15, 20, 30, and 40 kHz, at an amplitude of 10 V (peak). A square waveform with a duty cycle of 50% with no interphase delay was used. Stimulations of the pudendal nerve were carried out unilaterally and bilaterally in a randomized manner. Each frequency and voltage combination was applied once unilaterally to the left or right pudendal nerve and also bilaterally in each animal.

During all high-frequency stimulation experiments, the proximal electrode alongside the nerve was used to induce an anal sphincter contraction (square wave, 20 Hz, 3 V, 20% duty cycle, no interphase delay) for 2 seconds, 20 seconds, or 2 minutes. Thereafter, the high-frequency stimulation (square wave, 3–40 kHz, 10 V (peak), 50% duty cycle, no interphase delay) was turned on for 10 seconds with the distal electrode, whilst low-frequency stimulation continued through the proximal electrode. There was a rest period of 2 minutes between stimulation trials.

Outcome measures

The outcome measures during stimulation were: anal pressure, anal pressure change compared to baseline, and the relative change of anal pressure. The Matlab script that was used to compute these outcome measures is described in Suppl. C. The following equations were used:

Pressure change = peak pressure – mean baseline pressure (Figs 6 and 7)

Pressure change (onset response) = pressure end onset-pressure start onset (Fig. 10)

$$\textit{Relative pressure change} = \frac{\text{(pressure at the end of high frequency stimulation – mean baseline pressure)} - \text{(peak pressure during low frequency stimulation – mean baseline pressure)}}{\text{(peak pressure during low frequency stimulation – mean baseline pressure)}} \times 100\% \text{ (Fig. 9)}$$

Data collection and analysis

Anal pressure was recorded during rest and during electrical stimulation. Both pressure and stimulation signals were recorded using LabView©. Matlab© was used to compute the raw data into pressure values (in cmH_2O) and calculate the outcome measures. Statistical analysis was performed in SPSS©. Potential outliers were removed by using stem-and-leaf plots. The Shapiro–Wilk test was used to test for normality. A repeated-measures ANOVA, Friedman test, or Wilcoxon signed-rank test was applied to test for statistical significance. When a statistically significant result was detected with the Friedman test, a *post-hoc* Wilcoxon signed-rank test was applied to examine where the differences occurred. A p-value < 0.05 was considered statistically significant. For the *post-hoc* analyses, a Bonferroni correction was used to set the significance level. Results are presented as mean ± SEM.

Results

In silico *simulations*

Fig. 2 shows the propagation of action potentials when a single pulse and a pulse train of KHFAC stimulation at two amplitudes are simulated. The figure shows the situation when no block occurs, when a partial block occurs, and when a complete block occurs. The performance of a square wave was compared to the performances of sine and triangular waveforms (Fig. 3). Below 15 kHz, the block thresholds are relatively close together. However, due to the shape of the sine and triangular waveforms, the amount of charge that is injected in a single anodic or cathodic phase is significantly lower. Above 15 kHz, the block thresholds of the triangular and sine increase faster than the block threshold of the square wave; this results in the fact that the block threshold charges per phase of all three waveforms at the block threshold converge towards each other. Thus, the preferred waveform depends on whether a low block threshold or a low charge per phase is preferred.

Fig. 3 (c–f) shows the results for simulations with increasing interphase delays following anodal pulses ('anodal interphase delays') and cathodal pulses ('cathodal interphase delays') of a square wave with symmetrical anodal and cathodal pulses. Fig. 3c reveals that the block threshold rises exponentially after the sum of both interphase delays hits 60% of the total wave-period, yet it is mostly constant for values of the interphase delays that stay below 60% of the total wave-period. Apparently, the length of the anodal and cathodal pulses can be reduced significantly by introducing interphase delays, without having to increase the amplitudes of the pulses. This results in a decrease of the block threshold charge per phase, as seen in Fig. 3d. In other words: introducing interphase delays can lead to safer stimulation with nearly equal efficacy and power consumption. This effect is further studied in Fig. 3e and 3f. These figures are nearly symmetric in the line drawn by $T_{ipd\_anodal} = T_{ipd\_cathodal}$ (T_{ipd_anodal} = anodal interphase delay; $T_{ipd\_cathodal}$ = cathodal interphase delay), suggesting that increasing or decreasing the anodal interphase delay will have almost the same effect on the block threshold and corresponding charge per phase as increasing or decreasing the cathodal interphase delay. It also implies that in a bipolar set-up, the effect on the performance of the KHFAC signal at the anode and cathode of the electrode array will be equal.

Figs 4a and 4b show the influence of the electrode-to-axon distance on the block threshold and required charge per phase. This figure shows how much impact the electrode-to-axon distance has when designing a KHFAC therapy for the human pudendal nerve. Fig. 4a shows that for the axon at the furthest distance (about 5.84 mm), the block threshold is over 600 times larger than the block threshold for the axon closest to the electrode. Whereas if only half of the nerve needs to be blocked, the block threshold is 100 times larger than for the axon closest to the electrode.

In the following experiments, the return electrode, through which the current flows in the opposite direction, was placed at varying distances from the active electrode; this distance is called the 'interpolar distance'. In Figs 4c and 4d, the results of two electrode array (lead) orientations are shown:

- A parallel orientation, meaning that both electrodes are placed in such a way that the line connecting them is parallel to the axon.
- A perpendicular orientation, where one electrode is placed above the axon (the anode) and the other electrode is placed away from the axon in the x-direction (the cathode),

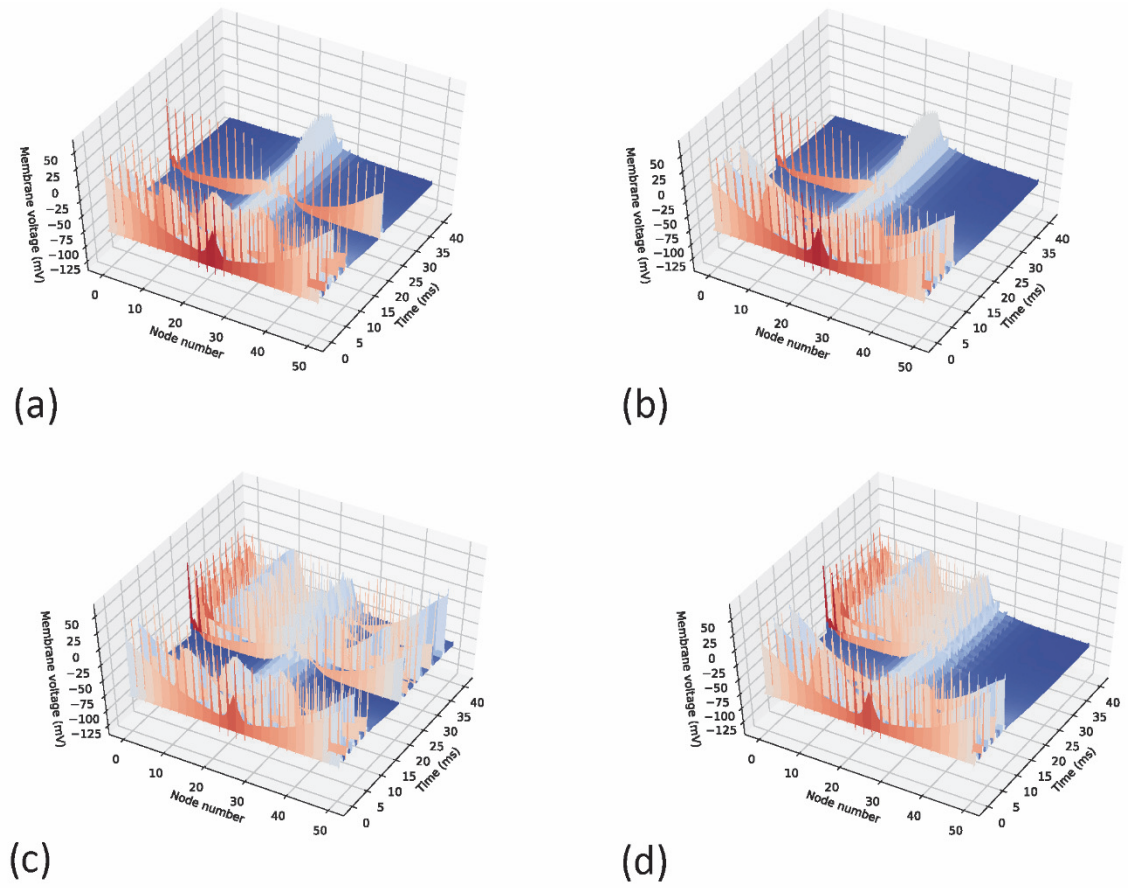

Fig. 2. Four different KHFAC block-determination simulations. The axon is modelled to consist of 51 nodes of Ranvier, with a 10 μm axon diameter. The KHFAC signal for each simulation is sinusoidal with a frequency of 20 kHz, and is initiated directly above the middle node at a distance of 1 mm. The simulation time step size used was 0.001 ms. (**a**) A KHFAC signal with a 0.53 mA amplitude is initiated at t = 0 ms. A single test pulse is delivered at node 0 at t = 20 ms. The block is unsuccessful. (**b**) A KHFAC signal with a 0.6 mA amplitude is initiated at t = 0 ms. A single test pulse is delivered at node 0 at t = 20 ms. The block is successful. (**c**) A KHFAC signal with a 0.53 mA amplitude is initiated at t = 0 ms. A pulse train starts from node 0 at t = 20 ms. Close inspection shows that the block is slightly successful, with a few pulses not reaching the other end of the axon. (**d**) A KHFAC signal with a 0.6 mA amplitude is initiated at t = 0 ms. A pulse train starts from node 0 at t = 20 ms. The block is 100% successful.

in such a way that the line between the two electrodes is perpendicular in the xy-plane.

The results show that in the mentioned set-up, for an interpolar distance of more than 7 mm, the block threshold and corresponding charge per phase converge to values that are also required in a monopolar set-up. The electric field at 1000 μm distance from the anode is thus perceived as equal to the electric field of a monopole. Below 7 mm, however, the block threshold has a reduction of more than 0.05 mA for the parallel setup. In the perpendicular set-up, this improvement is nullified, and the block thresholds and corresponding charges per phase only become worse for smaller interpolar distances.

Fig. 4e reveals the results of simulating different electrode orientations, both for the electrodes oriented at an angle in the xy-plane (towards the x-axis), and oriented at an angle in the yz-plane (towards the z-axis). The block threshold stays mostly equal when the angle in the xy-plane is below 10°. The block threshold does increase when a 10° angle is made in the zy-plane.

To achieve a better understanding of how the block threshold can be reduced for axons that lie at different distances from the electrode across the pudendal nerve, a simulation experiment was done, where both variables – electrode-to-axon distance and interpolar distance – were changed. The results are shown in Fig. 5, and reveal a combination of two effects:

- the quadratic effect of the electrode-to-axon distance, which was shown in Figs 4a and 4b;
- the effect of the interpolar distance, which was described in Figs 4c and 4d.

For higher electrode-to-axon distances, the reduction of block threshold that an optimized interpolar distance can cause, increases rapidly. Fig. 5 also reveals that the block thresholds are lowest with interpolar distances below 10 mm.

Low-frequency stimulation of the pudendal nerve

Proximal low-frequency stimulation of the pudendal nerve was applied to increase anal pressure that thereafter could be decreased by distal high-frequency stimulation (Fig. 6a). The average anal pressure without stimulation was (15.2 ± 2.1) cmH_2O. The average increase of anal pressure during unilateral stimulation at 10–30 Hz was (3.0 ± 0.8) – (15.2 ± 3.4) cmH_2O (Fig. 6b). There was a statistically significant difference in change of anal pressure during low-frequency stimulation depending on the frequency, chi-square (2) = 19.918, $p < 0.001$

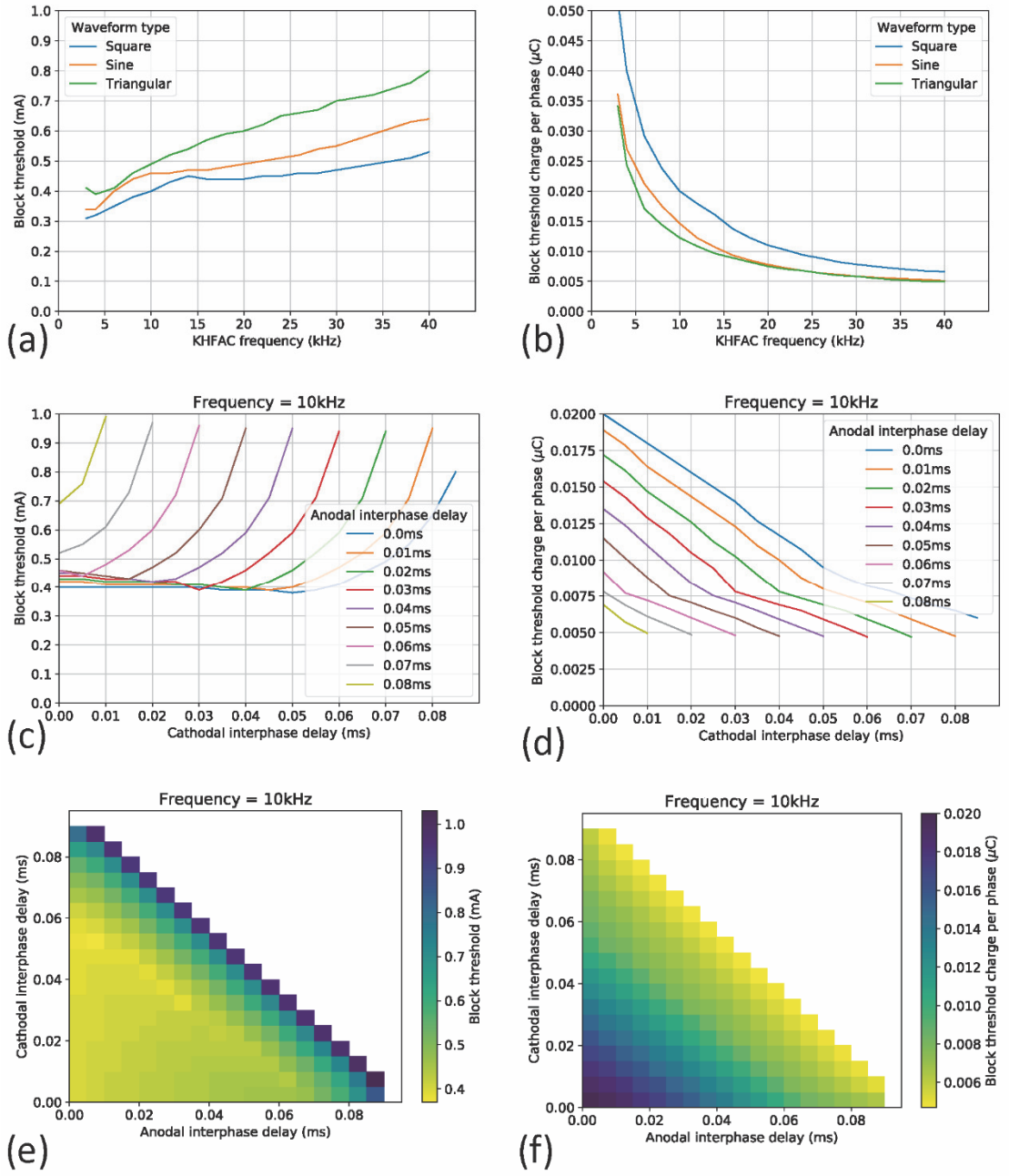

Fig. 3. Comparison of the performance of different waveforms for frequencies ranging from 3 to 40 kHz, and the effect of interphase delay (**a**) The block threshold of square, sine, and triangular waveforms. (**b**) The block threshold charge per phase of square, sine and triangular waveforms. (**c–d**) The influence of the addition of interphase delays on the performance of a 10 kHz square waveform. The time of the interphase delays are subtracted from the signal period; the remaining time is split between the anodal and cathodal pulse; this ensures that the frequency of the waveform remains intact. The anodal interphase delay is the interphase delay following the anodal (positive) pulse; the cathodal interphase delay is the interphase delay following the cathodal (negative) pulse. (**c**) The block thresholds for the different interphase delays. (**d**) The block threshold charges per phase for different interphase delays, the required charge per phase decreases linearly with a larger total interphase delay. (**e**) The block threshold for different interphase delays shows as pseudo-color plot. (**f**) The block threshold charge per phase for different interphase delays shown as pseudo-color plot.

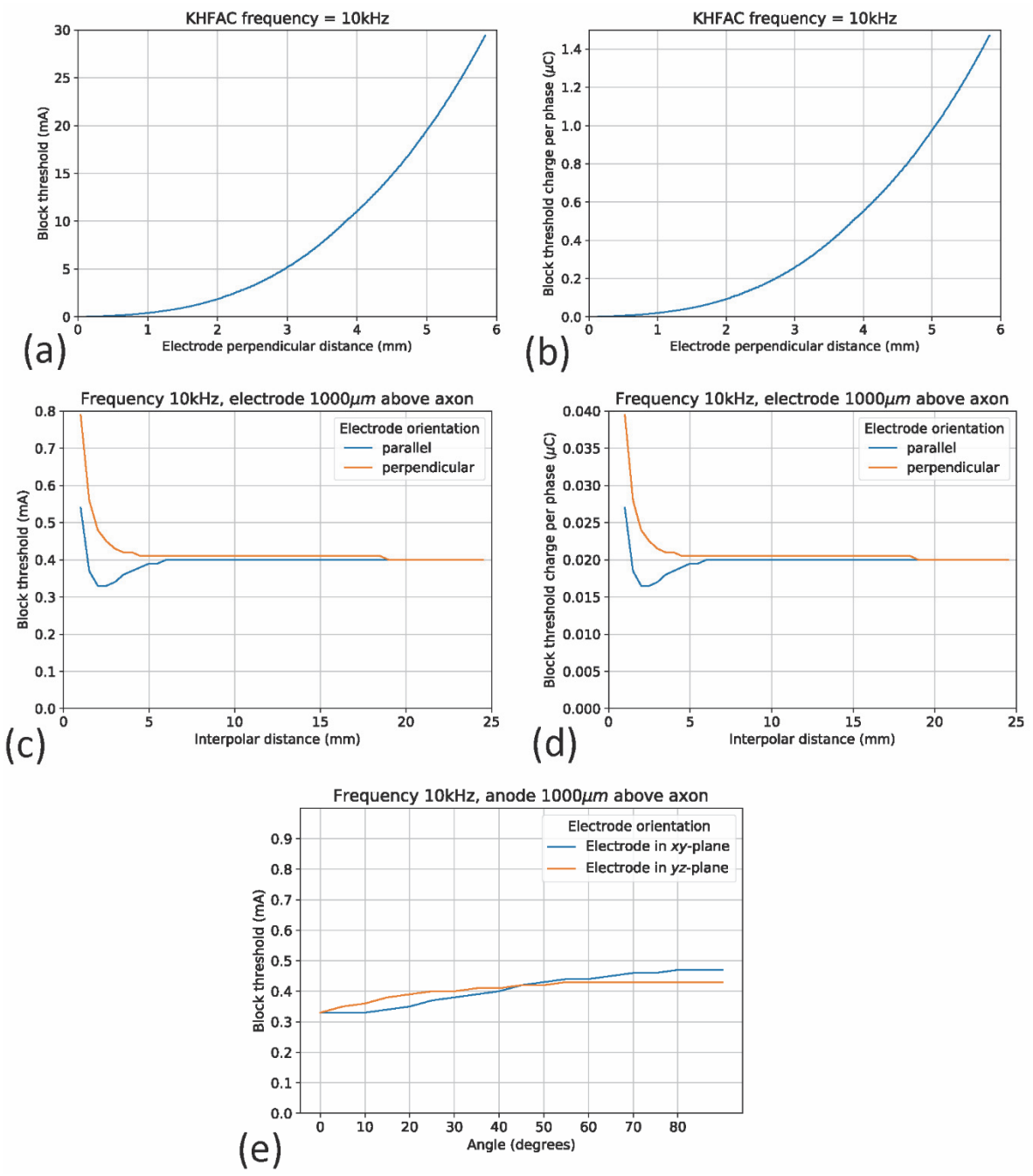

Fig. 4. The effects of electrode-to-axon distance, interpolar distance, and electrode orientation on block threshold. The signal is a 10 kHz symmetrical square wave. (**a**) The block threshold for increasing electrode-to-axon distance. (**b**) The block threshold charge per phase for increasing electrode-to-axon distance. (**c**) The block threshold for different interpolar distances of a bipolar set-up parallel and perpendicular to the axon. (**d**) The block threshold charge per phase for different interpolar distances of a bipolar set-up parallel and perpendicular to the axon. (**e**) The block threshold for two changing bipolar electrode orientations and an interpolar distance of 2200 μm.

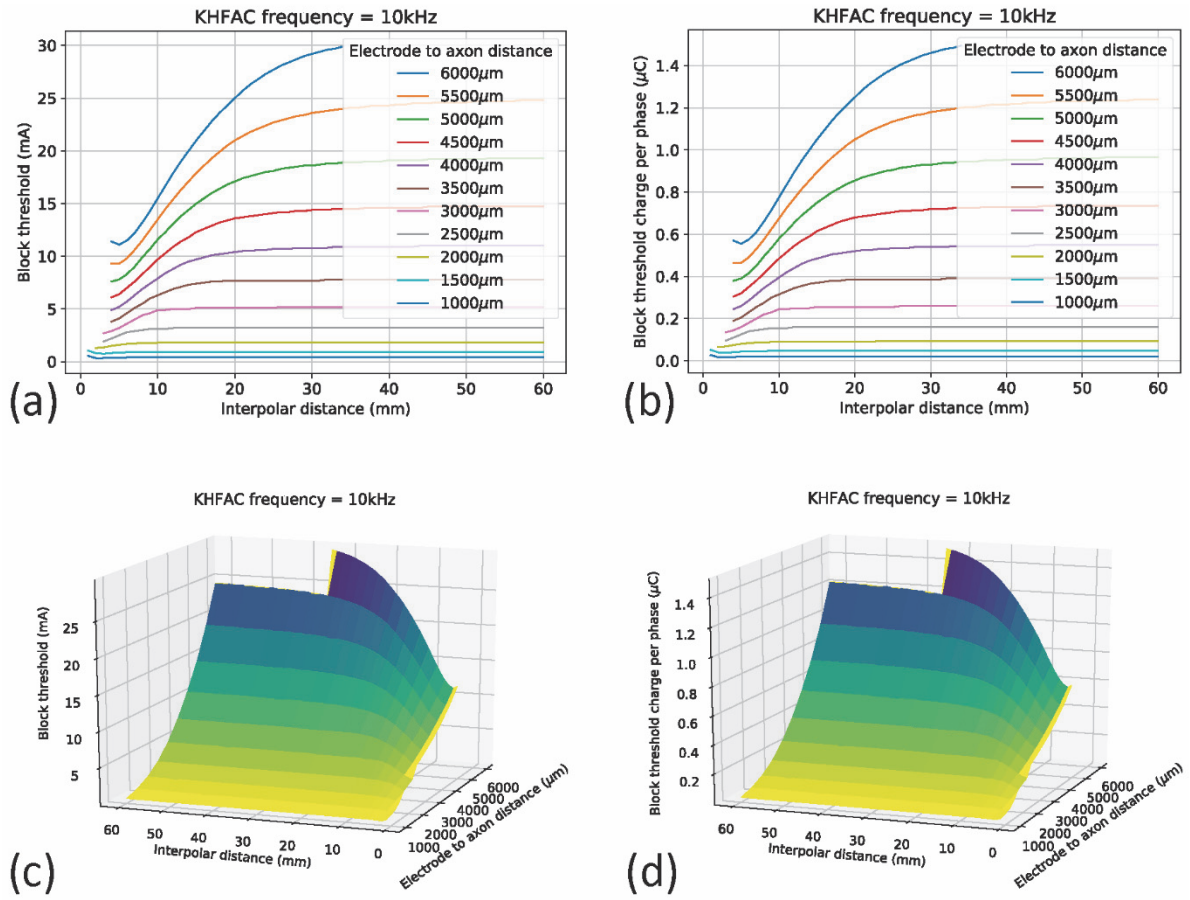

Fig. 5. The performance of different interpolar distances for increasing electrode-to-axon distances for a 10 kHz symmetrical square wave. (**a**) The block threshold. (**b**) The block threshold charge per phase. (**c, d**) The block threshold and block threshold charge per phase shown in a 3D plot, visualizing the relationship between interpolar distance and electrode-to-axon distance.

(Fig. 6b). *Post-hoc* analysis with a Wilcoxon signed-rank test was conducted with a Bonferroni correction applied, resulting in a significance level set at $p < 0.025$. This revealed a significant difference in anal pressure increase between 10 Hz and 20 Hz ($p = 0.001$), but not between 20 Hz and 30 Hz ($p = 0.096$).

When varying the amplitude between 1 V and 5 V of a unilaterally applied 20 Hz stimulus, the average anal pressure increase was (1.9 ± 0.7) – (15.1 ± 3.3) cmH_2O (Fig. 6d). There was a significant difference in anal pressure increase between different amplitudes (1–5 V) of stimulation, chi-square (4) = 42.577, $p < 0.001$ (Fig. 6d). *Post-hoc* analysis with a Wilcoxon signed-rank test was conducted with a Bonferroni correction applied, resulting in a significance level set at $p < 0.013$. These *post-hoc* analyses showed statistically significant differences between 1 V and 2 V ($p = 0.004$) and between 2 V and 3 V ($p = 0.002$). There were no significant differences between 3 V and 4 V ($p = 0.230$) and between 4 V and 5 V ($p = 0.180$).

Bilateral pudendal nerve stimulation with 10–30 Hz gave an average increase of anal pressure of (1.9 ± 0.9) – (11.5 ± 4.1) cmH_2O (Fig. 6c). The anal pressure was significantly different when comparing 10 Hz, 20 Hz and 30 Hz, chi-square (2), $p = 0.018$ (Fig. 6c). For the *post-hoc* analysis the significance level was set at $p < 0.025$. There were statistically significant differences between 10 Hz and 20 Hz ($p = 0.018$), but not between 20 Hz and 30 Hz ($p = 0.396$).

Bilateral pudendal nerve stimulation at 20 Hz with different amplitudes resulted in an average anal pressure increase of (1.5 ± 1.1) – (10.2 ± 2.5) cmH_2O (Fig. 6e). There was a significant difference in anal pressure change between the different amplitudes (1–5 V) of bilateral low-frequency pudendal nerve stimulation at 20 Hz, chi-square (4) = 20.824, $p < 0.001$ (Fig. 6e). For the *post-hoc* analysis the significance level was set at $p < 0.013$. *Post-hoc* analysis revealed no significant differences between 1 V and 2 V ($p = 0.039$), 2 V and 3 V ($p = 0.034$), 3 V and 4 V ($p = 0.498$), and 4 V and 5 V ($p = 0.408$).

Low-frequency stimulation at 20 Hz was carried out for 2, 20 and 120 seconds, unilaterally and bilaterally, to determine when the anal sphincter starts to fatigue (Fig. 7). During unilateral 20 Hz stimulation, the average change of anal pressure was (1.3 ± 0.4) cmH_20 during 2 seconds, and (–0.25 ± 0.5) cmH_2O during 120 seconds of stimulation (Fig. 7a). This change of anal pressure was significantly different when comparing activation during 2, 20 and 120 seconds, chi-square (2) = 6.565, $p = 0.038$ (Fig. 7a). For the *post-hoc* analyses, the significance level was set at $p < 0.025$. There were no significant differences in the average anal pressure increase between 20 seconds and 2 seconds of activation ($p = 0.805$) and between 120 second and 20 seconds of activation ($p = 0.038$). The average change in anal pressure was (4.2 ± 0.8) cmH_2O during 2 seconds of bilateral stimulation with 20 Hz and (2.5 ± 1.3) cmH_2O during 120 seconds of bilateral stimulation (Fig. 7b). Bilateral stimulation did not result in statistically significant changes in anal pressure when comparing 2, 20 and 120 seconds of stimulation, chi-square (2) = 4.275, $p = 0.118$ (Fig. 7b).

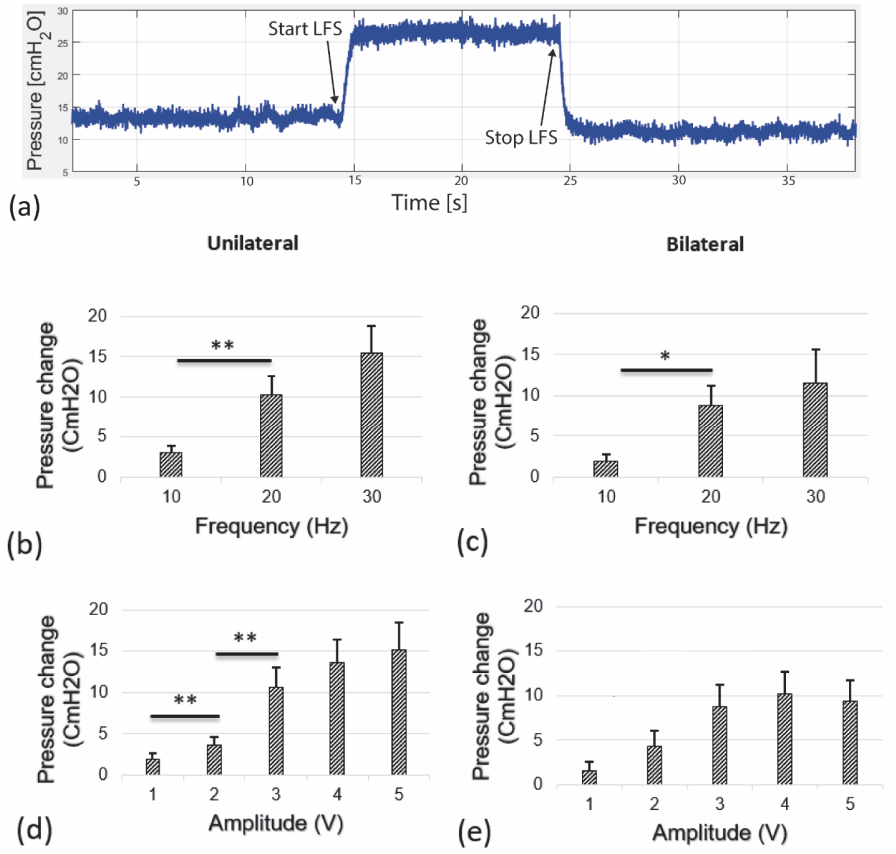

Fig. 6. Low-frequency stimulation of the pudendal nerve increases anal pressure. (**a**) Recording of anal pressure during unilateral pudendal nerve stimulation with a square wave, a frequency of 20 Hz, a 3 V amplitude, a 20% duty cycle, and no interphase delay. (**b**) Unilateral stimulation of 10–30 Hz with an amplitude of 3 V (n = 16 stimulations of 13 pudendal nerves). (**c**) Bilateral stimulation of 10–30 Hz (n = 7 stimulation of 5 rats). (**d**) Unilateral stimulation with a stimulus of 20 Hz with amplitudes ranging from 1 V – 5 V (n = 15 stimulation of 12 pudendal nerves). (**e**) Bilateral stimulation with a stimulus of 20 Hz with amplitudes ranging from 1–5 V (n = 7 stimulations of 5 rats). Mean, error bars represent SEM. * = $p < 0.05$; ** = $p < 0.01$. LFS = low-frequency stimulation.

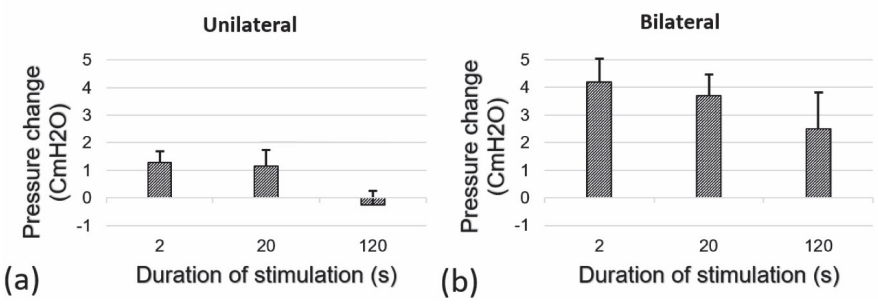

Fig. 7. Low-frequency stimulation (square wave, 20 Hz, 3 V amplitude, 20% duty cycle, no interphase delay) of the pudendal nerve for a duration of 2 seconds, 20 seconds and 120 seconds. (**a**) Unilateral stimulation during 2 seconds, 20 seconds, and 120 seconds (n = 25 stimulations of 5 pudendal nerves). (**b**) Bilateral stimulation during 2 seconds, 20 seconds, and 120 seconds (n = 15 stimulations in 3 rats). Mean, error bars represent SEM.

For the following high-frequency stimulation experiments, a stimulus with a square waveform, a frequency of 20 Hz with an amplitude of 3V, a 20% duty cycle, no interphase delay, and for a duration of 12 seconds was chosen for activation of the nerve based on the low-frequency stimulation results.

High-frequency stimulation of the pudendal nerve

During pilot experiments, high-frequency stimulation was applied distal to the application of low-frequency stimulation. After cessation of high-frequency stimulation, low-frequency stimulation continued for two seconds to determine whether a possible pressure decrease was likely due to nerve block or neurotransmitter depletion at the motor endplate. An example of these experiments is shown in Suppl. D. This figure shows that anal pressure increases during continued low-frequency stimulation, directly after cessation of high-frequency stimulation.

In the high-frequency stimulation experiments, a proximal stimulus at a frequency of 20 Hz was applied. Two seconds later a high-frequency stimulus in the range of 3 to 40 kHz was switched on distally from the first stimulus along the pudendal nerve. This stimulus had a duration of 10 seconds, a square waveform, an amplitude of 10 V and a duty cycle of 50%. Fig. 8a shows two recordings of anal pressure during such an experiment. The top graph shows anal pressure during unilateral low-frequency and high-frequency stimulation and the bottom graph shows anal pressure during bilateral low-frequency and high-frequency stimulation.

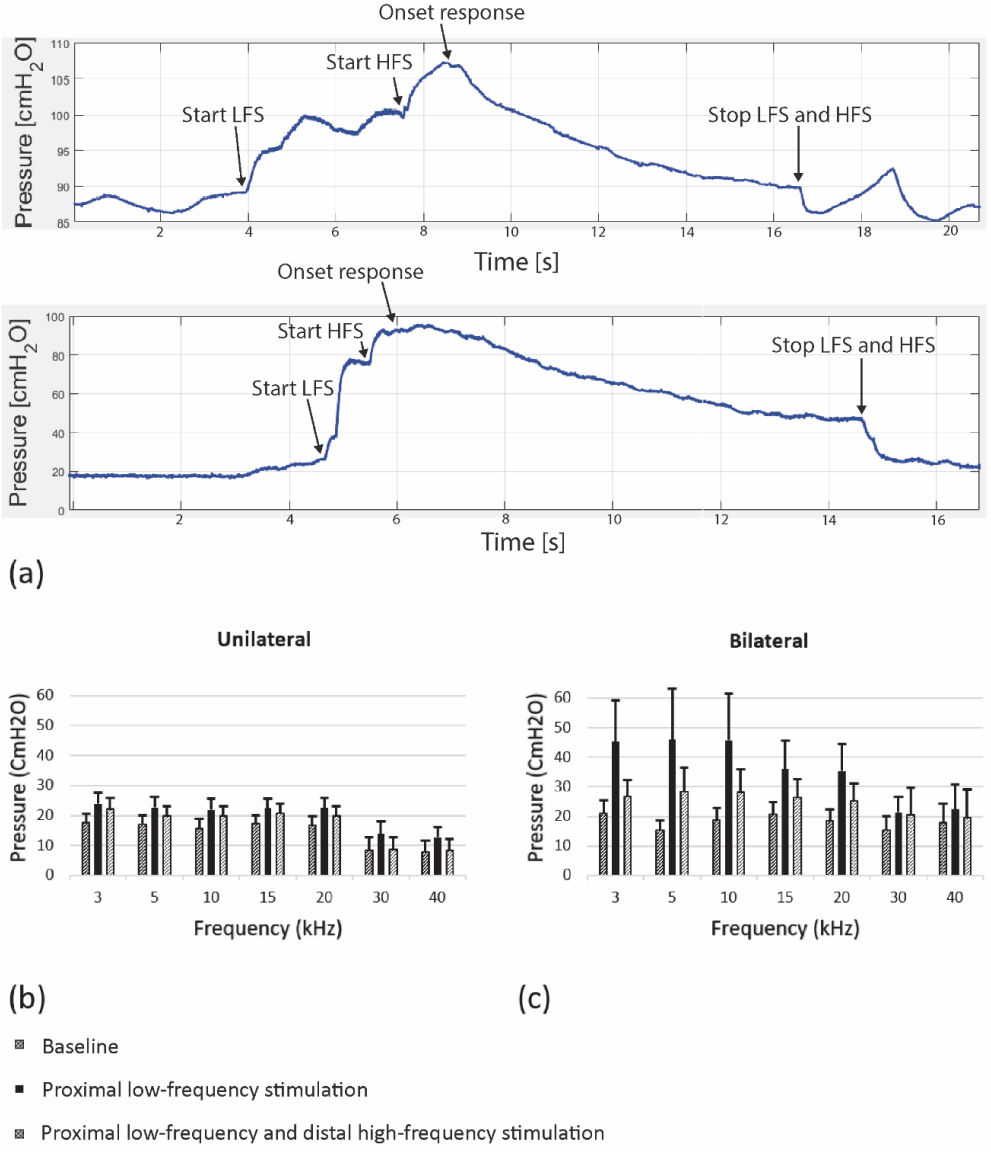

Fig. 8. The average anal pressure during baseline, proximal low-frequency and distal high-frequency stimulation of the pudendal nerve. (**a**) Recording of anal pressure during unilateral (top graph) and bilateral (bottom graph) proximal low-frequency stimulation (square wave, 20 Hz, 3 V amplitude, 20% duty cycle, no interphase delay) and distal high-frequency stimulation (square wave, 5 kHz, 10 V amplitude, 50% duty cycle, no interphase delay). (**b**, n = 25 stimulations of 18 pudendal nerves) The average anal pressure during baseline, proximal low-frequency stimulation, and distal high-frequency stimulation at 3–40 kHz during unilateral stimulation. (**c**, n = 4 stimulations in 3 rats) the average anal pressure during bilateral proximal low-frequency and distal high-frequency stimulation at 3–40 kHz. Mean, error bars represent SEM. HFS = high-frequency stimulation; LFS = low-frequency stimulation.

Fig. 8b–c depict the average anal pressure (in cmH_2O) during baseline, proximal low-frequency stimulation and distal high-frequency stimulation with a stimulus of 3, 5, 10, 15, 20, 30, or 40 kHz applied unilaterally and bilaterally. The average anal pressure during unilateral KHFAC stimulation was significantly lower than the average peak anal pressure during low-frequency stimulation (Wilcoxon signed-rank test, $p < 0.001$, $n = 167$ stimulations of 18 pudendal nerves at 3–40 kHz). Similarly, during bilateral KHFAC stimulation, the average anal pressure was significantly lower than the average peak anal pressure during low-frequency stimulation (Wilcoxon signed-rank test, $p < 0.001$, $n = 34$ stimulations in 3 rats at 3–40 kHz). During unilateral high-frequency stimulation, the average relative anal pressure decreased by (32 ± 18) – (96 ± 13)% when comparing the rats in which we applied frequencies of 3–40 kHz (Fig. 9a). During bilateral high-frequency stimulation, the average relative anal pressure decreased by (23 ± 69) – (92 ± 67)% when comparing the rats in which we applied frequencies of 3–40 kHz (Fig. 9b).

Onset response

The onset response is defined as the increase of anal pressure directly after the start of the high-frequency stimulus. Fig. 8a shows two examples of an onset response. The average change in anal pressure during the onset response ranged from (0 ± 0) – (3.5 ± 1.1) cmH_2O for frequencies from 3 to 40 kHz during unilateral proximal activation and distal kilohertz stimulation (Fig. 10a). The average change in anal pressure during the onset response ranged from (1.0 ± 1.0) – (3.8 ± 2.8) cmH_2O for frequencies of 3 to 40 kHz applied bilaterally (Fig. 10b).

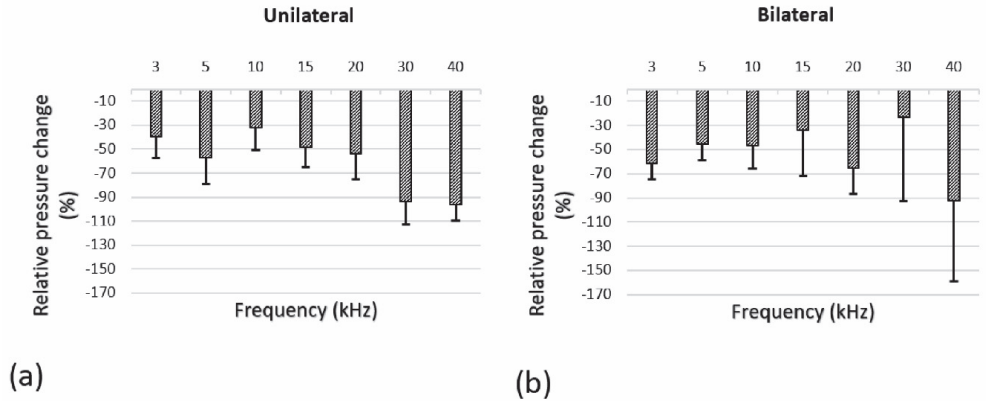

Fig. 9. The mean relative change of anal pressure during uni- and bilateral proximal low-frequency (square wave, 20 Hz, 3 V amplitude, 20% duty cycle, no interphase delay) and distal high-frequency stimulation (square wave, 10 V amplitude, 50% duty cycle, no interphase delay) of the pudendal nerve. (**a**) Unilateral proximal low-frequency stimulation and distal high-frequency stimulation from 3–40 kHz ($n = 25$ stimulations of 18 pudendal nerves). (**b**) Bilateral proximal low-frequency stimulation and distal high-frequency stimulation from 3–40 kHz ($n = 4$ stimulations in 3 rats).

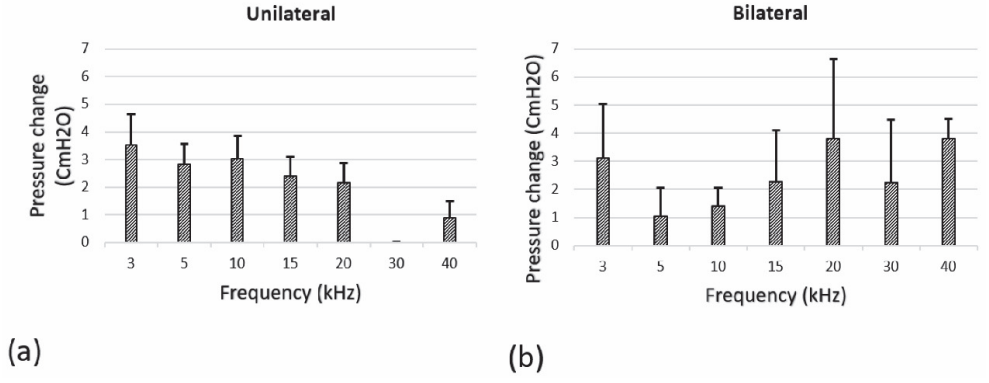

Fig. 10. The onset response at different frequencies. (**a**) Anal pressure change during the onset response after the start of unilateral high-frequency stimulation ($n = 23$ stimulations of 18 pudendal nerves). (**b**) Anal pressure change during the onset response after the start of bilateral high-frequency stimulation ($n = 4$ stimulations in 3 rats).

Discussion

With the simulations we aimed to determine which parameters influence the effectiveness of electrical pudendal nerve block induced by KHFAC neuromodulation. Previously the following parameters were tested: frequency, electrode-to-axon distance, axon diameter, a selection of different waveforms, temperature, and electrode surface (cuff electrodes) (Bhadra et al., 2007; Kilgore and Bhadra, 2014; Patel et al., 2017; Wang et al., 2008; Zhang et al., 2006; Zhao et al., 2015). However, not all of these studies included human axon models. Furthermore, all of the mentioned simulation studies only focus on monopolar set-ups (set-ups involving a return electrode placed at an infinite distance). One study utilized a bipolar set-up (a set-up involving a return electrode placed near the active electrode) to examine if block thresholds can be reduced by changing the interpolar distance (Ackermann et al., 2009b). However, only an electrode that was perfectly aligned at 1.0 mm above the axon was examined. Another previous study, including a bipolar cuff electrode, investigated the effect of waveform and duty cycle on block threshold, onset response, and power consumption (Peña et al., 2020). Thus far, studies have focused on the block threshold as a performance measure. However, the required charge per phase at the block threshold is just as important, as this is a measure of how many electrons are injected into the tissue. The amount of injected charge at the electrode-tissue interface should be minimized to prevent irreversible Faradaic reactions from occurring (Merrill et al., 2005).

Currently, chronic implants presume low power consumption, since replacing batteries requires surgery and wirelessly recharging implants are still only scarcely available. By reducing the block threshold, the required power for high-frequency stimulation can also be reduced. The simulations in this study showed that a square waveform can be chosen when a low amplitude is desired. Secondly, we show that the addition of interphase delays decreases the block threshold charge per phase but not the amplitude of the block threshold. Therefore, incorporating interphase delay in waveform design can increase safety without decreasing the effectiveness of the nerve block. Furthermore, choosing an interpolar distance and considering the alignment of the electrode can further optimize KHFAC stimulation.

In the present study, KHFAC neuromodulation of the pudendal nerve in the range of 3–40 kHz decreased anal pressure in rats, both unilaterally and bilaterally, during proximal low frequency stimulation of the pudendal nerve. Another aspect of high-frequency stimulation that must be taken into account is the onset response. The magnitude of the onset response seems to change with frequency, however no statistical tests were performed due to differences in group size. In previous reports, it has been shown that the onset response can be shortened by increasing the frequency (>20 kHz) and by optimizing electrode design (Ackermann et al., 2009a, 2010; Bhadra and Kilgore, 2005). A recent study investigated a theoretical model to eliminate the onset response (Yi and Grill, 2020). Future studies should also focus on determining the clinical relevance of the onset response when applying high-frequency stimulation to the pudendal nerve in patients.

We found no statistically significant differences in anal pressure during 2 seconds, 20 seconds and 2 minutes of stimulation with 20 Hz, 3 V. Previously it had been shown that the urethral sphincter in dogs fatigues between 15 and 20 seconds with 100–500 Hz stimulation with an amplitude of 3 V (Li et al., 1995). Thus, the results obtained with kilohertz-frequency stimulation starting after 2 seconds of low-frequency stimulation are not likely to be due to fatigue of the sphincter, but most likely represent nerve conduction block of the pudendal nerve or depletion of neurotransmitter at the motor endplate followed by relaxation of the pelvic musculature.

The effects of KHFAC neuromodulation have been investigated in various animal models, at multiple nerves. The proposed mechanism of action is that it induces nerve conduction block by inactivation/closure of sodium channels (Bhadra and Kilgore, 2004). This block of nerve conduction is rapid and reversible (Kilgore and Bhadra, 2004). This is a local block of nerve conduction at the site of the electrode rather than a depletion of neurotransmitter at the motor endplate (Williamson and Andrews, 2005). Bhadra et al. (2006) showed rapid onset and reversible motor block of the pudendal nerve with stimulation at frequencies of 1 to 30 kHz in cats.

Other studies in anesthetized cats, showed that a stimulus of 1 to 15 kHz applied to the pudendal nerve induced voiding (Cai et al., 2019; Gaunt and Prochazka, 2009; Yang et al., 2014). Several studies also showed that urethral pressure decreases during KHFAC stimulation of the pudendal nerves in cats and that this pressure decrease is reversible (Cai et al., 2019; Yang et al., 2014). Another study showed the inhibition of dyssynergic external urethral sphincter activity by 20 kHz stimulation of the pelvic nerves (Peh et al., 2018). Thus, the evidence that KHFAC neuromodulation induces conduction block comes mainly from simulation studies, whereas the studies performed in animal models provide evidence for the occurrence of a motor block.

A limitation of the present study is that healthy animals were used. No animal model for dyssynergic defecation exists. Secondly, the experiments were acute experiments that were performed under anesthesia and not in awake animals. Thirdly, the outcome measure that we used, anal pressure, is an indirect measure. It is not only a measure for anal sphincter muscle tone but also for other pelvic floor muscles. However, anal pressure is a clinically relevant outcome and, therefore, using this as an outcome did not impair our results. Another limitation is that the *in vivo* stimulations were done with a fixed voltage. The current that is delivered to the nerve depends on multiple factors, such as impedance of the electrode and tissue interface, which depends on for example frequency. We did not measure the current delivered to the nerve. Therefore, it is difficult to conclude which of the tested frequencies most efficiently decreased anal pressure.

We used commercially available electrode arrays for clinical use for stimulation of the pudendal nerve in the conducted animal experiments. Previous studies in animals used cuff electrodes to induce relaxation of the EUS. The insertion of a cuff electrode requires open surgery. In contrast, commercially available electrode arrays can be placed percutaneously under sedation or anesthesia in proximity to the target nerve in patients. Therefore, we conducted the present study to determine whether KHFAC neuromodulation is also able to induce a pressure decrease when using electrode arrays. The results obtained with electrode arrays imply that this technique effectively reduces anal pressure in rats. This technique might also be effective in patients with dyssynergic defecation. In the future, KHFAC neuromodulation of the pudendal nerves can be a good alternative for patients with failed treatments, such as optimizing fiber and fluid intake, laxatives, and biofeedback (Rao and Patcharatrakul, 2016). In some of these patients, however, the problem is a paradoxical contraction of the puborectal muscle, which is not innervated by the pudendal nerve. Pudendal high-frequency stimulation alone might not be effective in those patients.

Conclusions

Simulation models showed that a square waveform is the preferred waveform for KHFAC neuromodulation of the pudendal nerve when considering the block threshold. Incorporating an interphase delay can improve safety of the electrical nerve block. Furthermore, the alignment of the electrode along the nerve is an important factor to consider when a low block threshold is desired. *In vivo*, we showed in male and female rats that KHFAC neuromodulation of the pudendal nerve in the range of 3–40 kHz with an electrode array can effectively decrease anal pressure compared to that during low frequency stimulation of the pudendal nerve. This technique has the potential to improve defecation, micturition, and sexual function in patients with related dysfunction, such as dyssynergic defecation, urinary retention, and chronic pain in the genital and perigenital region.

Funding
This study is supported by Stichting Urologisch Wetenschappelijk Onderzoek (SUWO). The funding source had no involvement in study design, data collection, analysis, interpretation of the data, writing of the report, and submission of the article for publication.

Ethical aspects and conflict of interests
The authors have no conflict of interests to declare.

Acknowledgements
The authors would like to thank R. Guan and A. Kaichouhi (Section Bioelectronics, Delft University of Technology) for the technical support with designing and building the stimulator device.

References

Ackermann D, Foldes EL, Bhadra N, Kilgore KL (2009a). Electrode design for high frequency block: effect of bipolar separation on block thresholds and the onset response. Annu Int Conf IEEE Eng Med Biol Soc 2009: 654–657. DOI: 10.1109/IEMBS.2009.5332738.

Ackermann DM, Jr., Bhadra N, Foldes EL, Wang X-F, Kilgore KL (2010). Effect of nerve cuff electrode geometry on onset response firing in high-frequency nerve conduction block. IEEE Trans Neural Syst Rehabil Eng 18(6): 658–665. DOI: 10.1109/TNSRE.2010.2071882.

Ackermann DM, Jr., Foldes EL, Bhadra N, Kilgore KL (2009b). Effect of bipolar cuff electrode design on block thresholds in high-frequency electrical neural conduction block. IEEE Trans Neural Syst Rehabil Eng 17(5): 469–477. DOI: 10.1109/TNSRE.2009.2034069.

Bhadra N, Kilgore KL (2004). Direct current electrical conduction block of peripheral nerve. IEEE Trans Neural Syst Rehabil Eng 12(3): 313–324. DOI: 10.1109/TNSRE.2004.834205.

Bhadra N, Kilgore KL (2005). High-frequency electrical conduction block of mammalian peripheral motor nerve. Muscle Nerve 32(6): 782–790. DOI: 10.1002/mus.20428.

Bhadra N, Bhadra N, Kilgore K, Gustafson KJ (2006). High frequency electrical conduction block of the pudendal nerve. J Neural Eng 3(2): 180–187. DOI: 10.1088/1741-2560/3/2/012.

Bhadra N, Foldes EL, Ackermann D, Kilgore KL (2009). Reduction of the onset response in high frequency nerve block with amplitude ramps from non-zero amplitudes. Annu Int Conf IEEE Eng Med Biol Soc 2009: 650–653. DOI: 10.1109/IEMBS.2009.5332735.

Bhadra N, Lahowetz EA, Foldes ST, Kilgore KL (2007). Simulation of high-frequency sinusoidal electrical block of mammalian myelinated axons. J Comp Neurosci 22(3): 313–326. DOI: 10.1007/s10827-006-0015-5.

Bharucha AE, Wald A, Enck P, Rao S (2006). Functional anorectal disorders. Gastroenterology 130(5): 1510–1518. DOI: 10.1053/j.gastro.2005.11.064.

Cai H, Morgan T, Pace N, Shen B, Wang J, Roppolo JR, et al. (2019). Low pressure voiding induced by a novel implantable pudendal nerve stimulator. Neurourol Urodyn 38(5): 1241–1249. DOI: 10.1002/nau.23994.

Coolen RL, Groen J, Scheepe JR, Blok BFM (2020). Transcutaneous Electrical Nerve Stimulation and Percutaneous Tibial Nerve Stimulation to Treat Idiopathic Nonobstructive Urinary Retention: A Systematic Review. Eur Urol Focus 7(5): 1184–1194. DOI: 10.1016/j.euf.2020.09.019.

Gaunt RA, Prochazka A (2009). Transcutaneously coupled, high-frequency electrical stimulation of the pudendal nerve blocks external urethral sphincter contractions. Neurorehabil Neural Repair 23(6): 615–626. DOI: 10.1177/1545968308328723.

Hines ML, Carnevale NT (1997). The NEURON simulation environment. Neural Comput 9(6): 1179–1209. DOI: 10.1162/neco.1997.9.6.1179.

Kilgore KL, Bhadra N (2004). Nerve conduction block utilising high-frequency alternating current. Med Biol Eng Comput 42(3): 394–406. DOI: 10.1007/BF02344716.

Kilgore KL, Bhadra N (2014). Reversible nerve conduction block using kilohertz frequency alternating current. Neuromodulation 17(3): 242–255. DOI: 10.1111/ner.12100.

Lembo A, Camilleri M (2003). Chronic constipation. N Engl J Med 349(14): 1360–1368. DOI: 10.1056/NEJMra020995.

Li JS, Hassouna M, Sawan M, Duval F, Elhilali MM (1995). Long-term effect of sphincteric fatigue during bladder neurostimulation. J Urol 153(1): 238–242. DOI: 10.1097/00005392-199501000-00084.

McIntyre CC, Richardson AG, Grill WM (2002). Modeling the excitability of mammalian nerve fibers: influence of afterpotentials on the recovery cycle. J Neurophysiol 87(2): 995–1006. DOI: 10.1152/jn.00353.2001.

Merrill DR, Bikson M, Jefferys JGR (2005). Electrical stimulation of excitable tissue: design of efficacious and safe protocols. J Neurosci Methods 141(2): 171–198. DOI: 10.1016/j.jneumeth.2004.10.020.

Miles JD, Kilgore KL, Bhadra N, Lahowetz EA (2007). Effects of ramped amplitude waveforms on the onset response of high-frequency mammalian nerve block. J Neural Eng 4(4): 390–398. DOI: 10.1088/1741-2560/4/4/005.

Nyam DC, Pemberton JH, Ilstrup DM, Rath DM (1997). Long-term results of surgery for chronic constipation. Dis Colon Rectum 40(3): 273–279. DOI: 10.1007/BF02050415.

Patel YA, Kim BS, Rountree WS, Butera RJ (2017). Kilohertz electrical stimulation nerve conduction block: Effects of electrode surface area. IEEE Trans Neural Syst Rehabil Eng 25(10): 1906–1916. DOI: 10.1109/TNSRE.2017.2684161.

Peh WYX, Mogan R, Thow XY, Chua SM, Rusly A, Thakor NV, Yen SC (2018). Novel Neurostimulation of Autonomic Pelvic Nerves Overcomes Bladder-Sphincter Dyssynergia. Front Neurosci 12: 186. DOI: 10.3389/fnins.2018.00186.

Peña E, Pelot NA, Grill WM (2020). Quantitative comparisons of block thresholds and onset responses for charge-balanced kilohertz frequency waveforms. J Neural Eng 17(4): 046048. DOI: 10.1088/1741-2552/abadb5.

Rao SS, Patcharatrakul T (2016). Diagnosis and Treatment of Dyssynergic Defecation. J Neurogastroenterol Motil 22(3): 423–435. DOI: 10.5056/jnm16060

Rao SS, Bharucha AE, Chiarioni G, Felt-Bersma R, Knowles C, Malcolm A, Wald A (2016). Functional Anorectal Disorders. Gastroenterology 130(5): 1510–1518. DOI: 10.1053/j.gastro.2005.11.064.

Rao SS, Welcher KD, Leistikow JS (1998). Obstructive defecation: a failure of rectoanal coordination. Am J Gastroenterol 93(7): 1042–1050. DOI: 10.1111/j.1572-0241.1998.00326.x.

Smaragdos G, Chatzikonstantis G, Kukreja R, Sidiropoulos H, Rodopoulos D, Sourdis I, et al. (2017). BrainFrame: a node-level heterogeneous accelerator platform for neuron simulations. J Neural Eng 14: 066008. DOI: 10.1088/1741-2552/aa7fc5.

Tai C, Wang J, Wang X, Roppolo JR, de Groat WC (2007). Voiding reflex in chronic spinal cord injured cats induced by stimulating and blocking pudendal nerves. Neurourol Urodyn 26(6): 879–886. DOI: 10.1002/nau.20430.

van Asselt E, Choudhary M, Clavica F, van Mastrigt R (2017). Urethane anesthesia in acute lower urinary tract studies in the male rat. Lab Anim 51(3): 256–263. DOI: 10.1177/0023677216657850.

Wang J, Shen B, Roppolo JR, de Groat WC, Tai C (2008). Influence of frequency and temperature on the mechanisms of nerve conduction block induced by high-frequency biphasic electrical current. J Comput Neurosci 24(2): 195–206. DOI: 10.1007/s10827-007-0050-x.

Williamson RP, Andrews BJ (2005). Localized electrical nerve blocking. IEEE Trans Biomed Eng 52(3): 362–370. DOI: 10.1109/TBME.2004.842790.

Yang G, Wang J, Shen B, Roppolo JR, de Groat WC, Tai C (2014). Pudendal nerve stimulation and block by a wireless-controlled implantable stimulator in cats. Neuromodulation 17(5): 490–496. DOI: 10.1111/ner.12136.

Yi G, Grill WM (2020). Kilohertz waveforms optimized to produce closed-state Na+ channel inactivation eliminate onset response in nerve conduction block. PLoS Comput Biol 16(6): e1007766. DOI: 10.1371/journal.pcbi.1007766.

Zhang X, Roppolo JR, de Groat WC, Tai C (2006). Simulation analysis of conduction block in myelinated axons induced by high-frequency biphasic rectangular pulses. IEEE Trans Biomed Eng 53(7): 1433–1436. DOI: 10.1109/tbme.2006.873689.

Zhao S, Yang G, Wang J, Roppolo JR, de Groat WC, Tai C (2015). Conduction block in myelinated axons induced by high-frequency (kHz) non-symmetric biphasic stimulation. Front Comput Neurosci 9: 86. DOI: 10.3389/fncom.2015.00086.